PAPER Special Section on Discrete Mathematics and Its Applications

On Reconfiguring Radial Trees

Yoshiyuki KUSAKARI[†a)], ***Member***

SUMMARY A linkage is a collection of line segments, called bars, possibly joined at their ends, called joints. We consider flattening a tree-like linkage, that is, a continuous motion of their bars from an initial configuration to a final configuration looking like a"straight line segment," preserving the length of each bar and not crossing any two bars. In this paper, we introduce a new class of linkages, called "radial trees," and show that there exists a radial tree which cannot be flattened.

key words: *linkage,reconfiguration,straightening,flattening, monotone tree,radial tree.*

1. Introduction

A *linkage* is a collection of line segments, called *bars*, possibly joined at their ends, called *joints*. A *reconfiguration* of a linkage is a continuous motion of their bars, or equivalently a continuous motion of their joints, that preserves the length of each bar. Applications of this problem include robotics, hydraulic tube bending, and the study of macromolecule folding[3], [7]. A linkage is called *planar* if all bars are in the plane $\mathbb{R}^2$ with no intersection. A reconfiguration of a linkage is called *planar* if all bars are in the plane during the motion, and is called *non-crossing* if every two bars do not cross each other during the motion. In this paper, we consider only a planar reconfiguration of a planar linkage, and we may omit the word "planar." Furthermore, we consider only a non-crossing reconfiguration, and we may omit the word "non-crossing."

For such planar reconfiguration problems, there is a fundamental question: whether any polygonal chain can be "straightened." This problem has been known as *"The Carpenter's Rule Problem"* [3], [7], [8], and had been open from the 1970's to the 1990's. However, Connelly et al. have answered this question affirmatively: they showed that any polygonal chain can be straightened, and they gave a method for straightening polygonal chains[3]. Streinu gave another method for straightening polygonal chains[8]. Both methods above work well for "convexifying" closed polygonal chains (polygons).

For a non-crossing planar reconfiguration of tree-like linkages, several negative results are known, that is, there exist trees which cannot be "flattened" [2], [4],

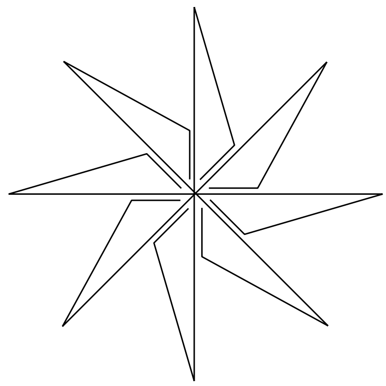

Fig. 1 A locked tree[2].

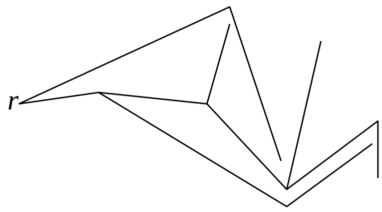

Fig. 2 A monotone tree [5].

[6]. Figure 1 illustrates a tree which cannot be flattened[2]. In Ref. [4], Connelly et al. gave a method for proving that some trees are locked, that is, cannot be flattened. On the other hand, an affirmative result was reported for reconfiguring tree linkages: Kusakari et al. showed that any "monotone tree" can be flattened, and gave a method for flattening "monotone trees" [5]. Figure 2 illustrates a monotone tree[5]. Recently, the complexity of flattening tree linkages has been studied: Alt et al. showed that deciding lockability for trees is PSPACE-complete[1]. However, there exist a few characterizations of tree linkages which can be flattened. Thus, it is desired to characterize a class of trees which can be flattened.

In this paper, we define a new class of trees, called "radially monotone trees" or "radial trees," which is a natural modification of the class of monotone trees, and show that there exists a radial tree which cannot be flattened. Figure 3 illustrates a locked radial tree. An early version of the paper was presented at a conference[6]. The remainder of this paper is organized as follows. In Sect. 2, we give some preliminary def-

†Department of Electronics and Information Systems, Faculty of Systems Science and Technology, Akita Prefectural University, Honjo Akita, 015-0055, Japan.
a) E-mail: kusakari@akita-pu.ac.jp

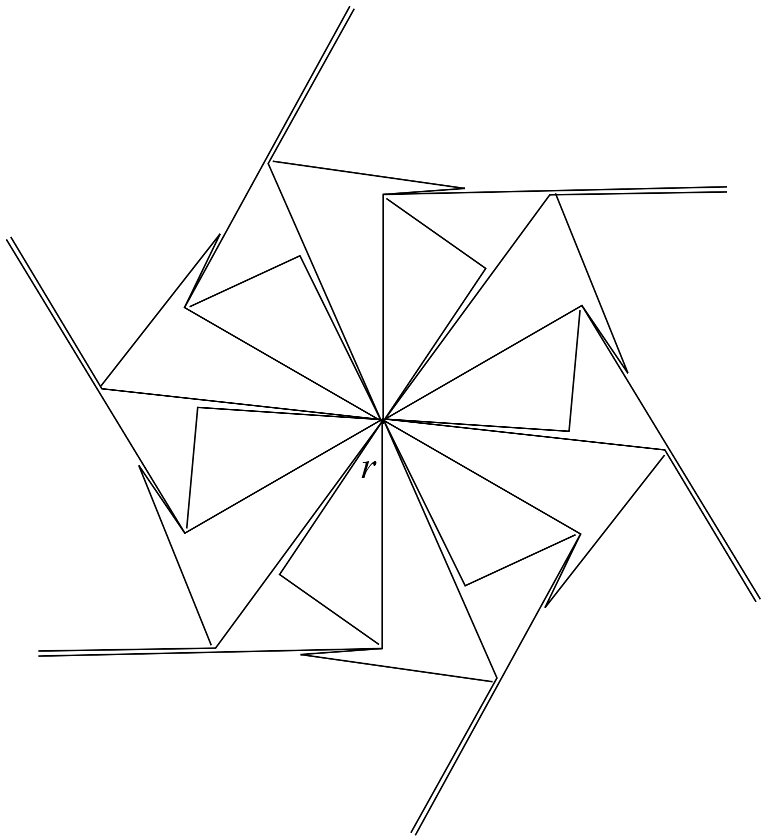

Fig. 3 An overview of a locked radial tree.

initions. In Sect. 3, we give a method to construct a locked radial tree. In Sect. 4, we show that the tree constructed in Sect. 3 is simple and radial. In Sect. 5, we present a theorem that the tree constructed in Sect. 3 cannot be flattened. In Sect. 6, we prove lemmas whose proofs are omitted in Sect. 5. We conclude in Sect. 7.

2. Preliminaries

Let $L = (J, B)$ denote a linkage consisting of a joint set J and a bar set B. A structural graph of a linkage L is denoted by $G(L)$. An embedding of a structural graph $G(L)$ is called a *configuration* of linkage L. A linkage L is called a *(rooted) tree linkage* or a *(rooted) tree* if the structural graph $G(L)$ is a (rooted) tree. Let $T = (J, B)$ be such a rooted tree linkage, and let $r \in J$ be the root of T. A bar $b \in B$ is denoted by (j_s, j_t) if $j_s \in J$ is the parent of $j_t \in J$. For any joint $j \in J$, a bar emanating from j, $b = (j, j')$, is called a *child bar of joint* j. A *leaf* is a joint having no child bar. For any joint $j \in J - \{r\}$, a bar entering to j, $b = (j', j)$, is called a *parent bar of joint* j. For any joint $j \in J - \{r\}$, a parent bar of j is unique, and is denoted by $\overline{j}$. A joint $j \in J$ is *internal* if j is neither the root nor a leaf. A *flattened configuration of a rooted tree linkage* is one in which the parent bar $\overline{j}$ of j makes angle π with each child bar of j for every internal joint j, and the angle between each pair of child bars of j is zero for every non-leaf joint $j \in J$. *Flattening a tree linkage* T is a reconfiguration of T from an initial configuration to a flattened configuration.

As an initial configuration of a tree linkage, we first define a monotone tree [5]. A polygonal chain P is *x-monotone* if the intersection of P and any vertical line is either a single point or a line segment if the intersection is not empty. A tree T is *x-monotone* if T is a rooted tree and every root-leaf polygonal chain in T is x-monotone. (See Fig. 2.)

Next, we define radial trees by slightly modifying the definition of monotone trees. A polygonal chain P is *radially monotone for a point* p (or, for short, *radial for a point* p) if the intersection of P and any circle with the same center p is either a single point or empty. A tree T is *radially monotone* or *radial* if T is a rooted tree and every root-leaf polygonal chain in T is radially monotone for the root r. A radial tree is illustrated in Fig. 3. On the other hand, the tree illustrated in Fig. 1 is not radial. Furthermore, every locked tree in [1], [2], [4] is not radial. Note that an x-monotone tree may not be radial, and a radial tree may not be x-monotone.

For three points $p_1, p_2, p_3 \in \mathbb{R}^2$, the angle $\angle p_1 p_2 p_3$ is measured counterclockwise at point p_2 from the direction of $\overrightarrow{p_2 p_1}$ to the direction of $\overrightarrow{p_2 p_3}$, and ranges in $[0, 2\pi)$. For two bars $\overline{j_1} = (j_0, j_1), \overline{j_2} = (j_1, j_2) \in B$

joined with joint j_1, the angle $\angle j_0 j_1 j_2$ is denoted by $\theta(\overline{j_1}, \overline{j_2})$. The *slope* $s(\overline{j_1})$ of bar $\overline{j_1} = (j_0, j_1)$ is the angle measured counterclockwise at the parent joint j_0 from $+x$ direction to the direction $\overrightarrow{j_0 j_1}$, and ranges in $[0, 2\pi)$. The length of bar $b \in B$ is denoted by $|b|$. For two points $p_1, p_2 \in \mathbb{R}^2$, the ray starting from p_1 and passing through p_2 is denoted by $R(p_1, p_2)$. For a point $p \in \mathbb{R}^2$ and a direction $d \in [0, 2\pi)$, the ray starting from p and going in the direction d is denoted by $R_p(d)$. The circle centered at $p \in \mathbb{R}^2$ with radius $a \in \mathbb{R}$ is denoted by $O_p(a)$, and the circle with diameter $p_1 p_2$ is denoted by $O(p_1, p_2)$.

3. Constructing a Locked Radial Tree

In this section, we construct a radial tree which cannot be flattened, i.e., we construct a *locked* radial tree. Figure 3 illustrates such a locked radial tree.

3.1 Outline of construction

In this subsection, we show how to construct a locked radial tree. We first define some terms on a locked radial tree. Figure 3 does not illustrate a strict locked radial tree. Some bars should be overlapped and some joints should be touched each other in a strict locked radial tree.

The locked tree T in Fig. 3 contains six congruent components C_0, C_1, $\cdots$, C_5, all of which are joined at the root r of T. More generally, one can construct a locked radial tree by such $n(> 4)$ congruent components, each of which is called a C_i *component* and is often denoted by C_i, for i, $0 \le i \le n-1$. Each C_i component consists of three subcomponents: a V_i *component*, an L_i *component* and a Γ_i *component*. These V_i, L_i and Γ_i components are often denoted by V_i, L_i and Γ_i, respectively. For each i, $0 \le i \le n-1$, these V_i, L_i and Γ_i are incident to the root r counterclockwise in this order. Furthermore, L_i is wrapped by V_i and Γ_i, as illustrated in Fig. 4.

The V_i component has two bars $\overline{v_1} = (v_0, v_1)$ and $\overline{v_2} = (v_1, v_2)$, joined with the internal joint v_1, whose angle $\theta(\overline{v_1}, \overline{v_2})$ is equal to $\frac{\pi}{2} + \frac{\pi}{n} (= \frac{\pi}{2} + \frac{\pi}{6})$, and V_i looks like the letter "V", as illustrated in Fig. 5.

The L_i component has two bars $\overline{l_1} = (l_0, l_1)$ and $\overline{l_2} = (l_1, l_2)$, joined with the internal joint l_1, whose angle $\theta(\overline{l_1}, \overline{l_2})$ is equal to $\frac{3\pi}{2}$, and L_i looks like the letter "L", as illustrated in Fig. 6.

The Γ_i component has four bars $\overline{\gamma_1} = (\gamma_0, \gamma_1)$, $\overline{\gamma_2} = (\gamma_1, \gamma_2)$, $\overline{\gamma_3} = (\gamma_1, \gamma_3)$ and $\overline{\gamma_4} = (\gamma_3, \gamma_4)$, and two internal joints γ_1, γ_3. Γ_i looks like the letter "Γ", as illustrated in Fig. 7. The angles $\angle \gamma_0 \gamma_1 \gamma_2$, $\angle \gamma_0 \gamma_1 \gamma_3$ and $\angle \gamma_0 \gamma_3 \gamma_4$ are $\frac{\pi}{2}$, $\frac{\pi}{2}$ and $\frac{3\pi}{2}$, respectively.

3.2 Detail of construction

In this subsection, we focus on a single C_i component,

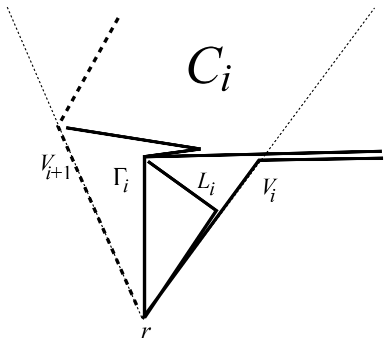

Fig. 4 Component C_i.

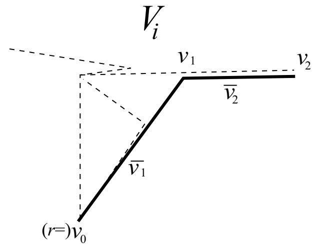

Fig. 5 Subcomponent V_i.

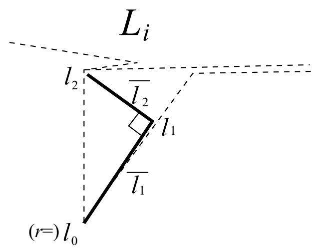

Fig. 6 Subcomponent L_i.

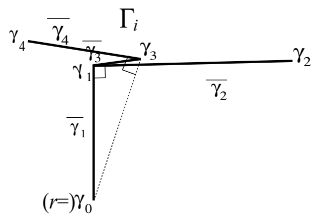

Fig. 7 Subcomponent Γ_i.

and may often omit the index i for simplicity. Furthermore, subcomponents, bars, and joints in C_{i-1} or C_{i+1} are designated by the corresponding objects with symbol "−" or "+", respectively. For example, Γ_{i-1}, Γ_i and Γ_{i+1} are denoted by Γ^-, Γ and Γ^+, respectively. Moreover, the bar in Γ_{i+1} corresponding to the bar $\overline{\gamma_1}$ in Γ_i is denoted by $\overline{\gamma_1}^+$. We use similar notation for the others. For two points $p_1, p_2 \in \mathbb{R}^2$, we denote by $p_1 p_2$ the line segment connecting p_1 and p_2, and by $|p_1 p_2|$ the length of the segment $p_1 p_2$.

We will define an initial configuration C_i^* of the C_i component. A joint $j \in J$ in C_i is denoted by j^* in C_i^*, and a bar $b \in B$ in C_i is denoted by b^* in C_i^*. For i, $0 \leq i \leq n-1$, we draw all figures C_i^* simultaneously so that each pair of corresponding bars in consecutive components makes angle $\frac{2\pi}{n}$, and the index i increases counterclockwise.

Without loss of generality, we may assume that the length $|\overline{\gamma_1}^*|$ is equal to 1, and the slope $s(\overline{\gamma_1}^*)$ is equal to $\frac{\pi}{2}$. Recall that we draw all bars corresponding to $\overline{\gamma_1}^*$ for all C_i^* simultaneously.

Then, for each i, $0 \leq i \leq n-1$, we draw line segments $\overline{\gamma_2}^* = \gamma_1^*\gamma_2^*$ on each ray $R_{\gamma_1^*}(0)$ from the point γ_1^*, so that the angle $\theta(\overline{\gamma_1}^*, \overline{\gamma_2}^*)$ is equal to $\frac{\pi}{2}$. We choose the length $|\overline{\gamma_2}^*|$ long enough, so that the ray $R(r, (\gamma_1)^{-*})$ intersects $\overline{\gamma_2}^*$. Thus, we choose the length $|\overline{\gamma_2}^*|$ so as to satisfy $|\overline{\gamma_2}^*| > \tan(\frac{2\pi}{n})$.

Next, we choose a point γ_4^* on the bar $(\overline{\gamma_2})^{+*}$, so that the following inequality holds:

$$\tan(\frac{\pi}{n}) < |\gamma_1^{+*}\gamma_4^*| < \min\{\tan(\frac{2\pi}{n}), \frac{1}{\sin(\frac{2\pi}{n})}\}. \quad (1)$$

The condition $\tan(\frac{\pi}{n}) < |\gamma_1^{+*}\gamma_4^*| < \tan(\frac{2\pi}{n})$ ensures that γ_4^* lies between points X and Y, which are defined later. (See Fig. 8.) Moreover, the condition $\tan(\frac{\pi}{n}) < |\gamma_1^{+*}\gamma_4^*| < \frac{1}{\sin(\frac{2\pi}{n})}$ ensures that γ_4^* lies between points W and Y, which are also defined later. (See Fig. 10.) Thus, inequality (1) ensures that γ_4^* is contained in both XY and WY.

One can find the point γ_3^*, on the bar $\overline{\gamma_2}^*$, satisfying $\angle\gamma_4^*\gamma_3^*r = \frac{\pi}{2}$. Actually, the point γ_3^* is the intersection of the bar $\overline{\gamma_2}^*$ and the circle $O(r, \gamma_4^*)$. Then, we draw two line segments γ_4^*r and $\gamma_4^*\gamma_3^*$. (See Fig. 10.)

We finally drop a perpendicular from γ_1^* to $rv_1^*(= r(\gamma_4)^{-*})$, and let l_1^* be the foot of the perpendicular.

We construct C_i on the figure C_i^*. For a joint j and a point p, the notation $j = p$ means that joint j is configured at point p. For a bar b and a line segment s, the notation $b = s$ also means that bar b is configured at line segment s. The initial configuration of the C_i component is obtained as follows. (See Figures 4-7, and 10.)

For the V_i component, let $v_1 = v_1^*(= (\gamma_4)^{-*})$, $v_2 = \gamma_2^*$, $\overline{v_1} = \overline{v_1}^*(= rv_1^*)$, and $\overline{v_2} = \overline{v_2}^*(= v_1^*\gamma_2^*)$.

For the L_i component, let $l_1 = l_1^*$, $l_2 = l_2^*(= \gamma_1^*)$, $\overline{l_1} = \overline{l_1}^*(= rl_1^*)$, and $\overline{l_2} = \overline{l_2}^*(= l_1^*l_2^*)$.

For the Γ_i component, $\gamma_1 = \gamma_1^*$, $\gamma_2 = \gamma_2^*$, $\gamma_3 = \gamma_3^*$, $\gamma_4 = \gamma_4^*(= v_1^{+*})$, $\overline{\gamma_1} = \overline{\gamma_1}^*(= r\gamma_1^*)$, $\overline{\gamma_2} = \overline{\gamma_2}^*(= \gamma_1^*\gamma_2^*)$, $\overline{\gamma_3} = \overline{\gamma_3}^*(= \gamma_1^*\gamma_3^*)$, and $\overline{\gamma_4} = \overline{\gamma_4}^*(= \gamma_3^*\gamma_4^*)$.

From this construction, one observes that $|\overline{v_1}| = |\overline{v_1}^*|$, $|\overline{v_2}| = |\overline{v_2}^*|$, $|\overline{l_1}| = |\overline{l_1}^*|$, $|\overline{l_2}| = |\overline{l_2}^*|$, $|\overline{\gamma_1}| = |\overline{\gamma_1}^*|$, $|\overline{\gamma_2}| = |\overline{\gamma_2}^*|$, $|\overline{\gamma_3}| = |\overline{\gamma_3}^*|$, and $|\overline{\gamma_4}| = |\overline{\gamma_4}^*|$. Note that all lengths $|\overline{\gamma_3}|$, $|\overline{v_1}|$, $|\overline{l_1}|$ and $|\overline{l_2}|$ are determined if $|\gamma_1^+\gamma_4|$ is determined.

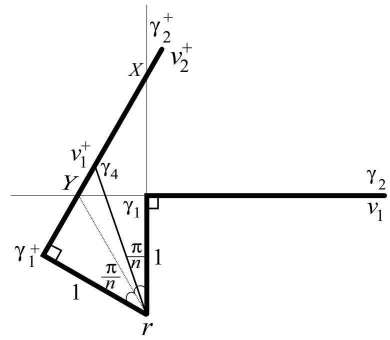

Fig. 8 Position of v_1^+.

4. The initial configuration

In this section, we show that the tree constructed in the previous section is simple and radial. From now on, we often do not distinguish the linkage and its configuration, and may often omit the symbol "*."

4.1 Simplicity

The slope $s(\overline{\gamma_2}^+)$ is equal to $\frac{2\pi}{n}$ and is smaller than $\frac{\pi}{2}$ if $n > 4$. The length $|\overline{\gamma_2}^*|$ is greater than $\tan\frac{2\pi}{n}$ from the construction. Therefore, the ray $R_{\gamma_1}(\frac{\pi}{2})$ should cross $\overline{\gamma_2}^+$. Let X be the intersection point of the ray $R_{\gamma_1}(\frac{\pi}{2})$ with $\overline{\gamma_2}^+$, and let Y be the intersection point of the ray $R_{\gamma_1}(\pi)$ with $\overline{\gamma_2}^+$, as illustrated in Fig. 8.

Since the length $|\overline{\gamma_1}^+|$ is equal to 1 and $\angle Xr\gamma_1^+$ is equal to $\angle\gamma_1 r\gamma_1^+(= \frac{2\pi}{n})$, the length $|\gamma_1^+X|$ is equal to $\tan(\frac{2\pi}{n})$. Furthermore, one can observe $|\gamma_1^+Y| = \tan(\frac{\pi}{n})$ as follows: since the hypotenuses are common and $|r\gamma_1| = |r\gamma_1^+|(= 1)$, the two right triangles $\triangle rY\gamma_1$ and $\triangle rY\gamma_1^+$ are congruent, and hence $\angle\gamma_1 rY = \angle Yr\gamma_1^+ = \frac{\pi}{n}$. Thus, the point γ_4^* is contained in the open line segment XY since the condition $\tan(\frac{\pi}{n}) < |\gamma_1^{+*}\gamma_4^*| < \tan(\frac{2\pi}{n})$ holds by construction. Therefore, one can observe that the two line segments $\gamma_4^*r(= (\overline{v_1})^{+*})$ and $\gamma_4^*\gamma_3^*(= \overline{\gamma_4}^*)$ can be drawn without (properly) crossing any other line segments. Furthermore, one can easily observe that any pair of line segments in C_i^* can be drawn without (properly) crossing even if the pair contains neither $(\overline{v_1})^{+*}$ nor $\overline{\gamma_4}^*$. Therefore, the tree constructed in Sect. 3 is simple.

4.2 Radial Monotonicity

For any joint $j \in J$, a subtree of T rooted at j is denoted by $T(j)$. A *fan* p_1jp_2 is the set of points swept out by a ray starting j moving counterclockwise from the direction $\overrightarrow{jp_1}$ to the direction $\overrightarrow{jp_2}$, and contains points on both $R(j, p_1)$ and $R(j, p_2)$. A fan p_1jp_2 may be denoted by $F_j[\theta_1, \theta_2]$, where $\theta_1 = \angle rjp_1$ and $\theta_2 = \angle rjp_2$. (See Fig. 9.)

The following lemmas hold.

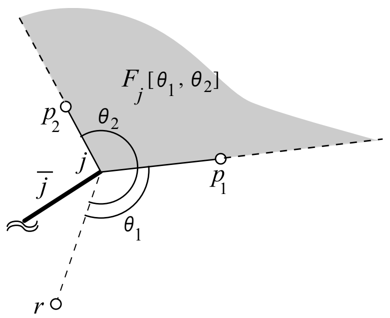

Fig. 9 Fan $F_j[\theta_1, \theta_2]$.

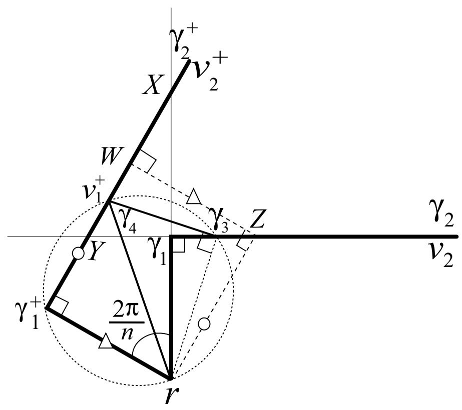

Fig. 10 Position of γ_3.

Lemma 1: (i) A tree $T = (J, B)$ is radial if and only if, for any joint $j \in J$, all points p (except for j) contained in the subtree $T(j)$ are properly outside of the circle $O_r(|rj|)$.
(ii) A tree $T = (J, B)$ is radial if and only if, for any joint $j \in J - \{r\}$, every child bar $b = (j, j') \in B$ is contained in the fan $F_j[\frac{\pi}{2}, \frac{3\pi}{2}]$.

Proof. Both (i) and (ii) are obvious from the definition of radial trees. □

Note that, for every bar $b = (r, j)$ emanating from the root r, the slope $s(b)$ can take any value in $[0, 2\pi)$ even if T is radial.

Lemma 2: (i) The V_i component is radial for the root r.
(ii) The L_i component is radial for the root r.
(iii) The Γ_i component is radial for the root r.

Proof. (i) One can easily observe that the angle $\theta(\overline{v_1}, \overline{v_2})$ is greater than or equal to $\frac{\pi}{2}$. (See Fig. 5.)

Thus, the bar $\overline{v_2}$ is contained in the fan $F_{v_1}[\frac{\pi}{2}, \frac{3\pi}{2}]$, and hence the path $(r =)v_0v_1v_2$ is radial by Lemma 1 (ii).
(ii) From the construction of the L_i component, the angle $\theta(\overline{l_1}, \overline{l_2})$ is equal to $\frac{3\pi}{2}$. Thus, the bar $\overline{l_2}$ is contained in $F_{l_1}[\frac{\pi}{2}, \frac{3\pi}{2}]$, and hence the path $(r =)l_0l_1l_2$ is radial by Lemma 1 (ii).
(iii) Since the Γ_i component has two leaves, it is sufficient to show that both path P_1 and path P_2 are radial, where $P_1 = \gamma_0\gamma_1\gamma_2$ and $P_2 = \gamma_0\gamma_1\gamma_3\gamma_4$. From the construction, $\theta(\overline{\gamma_1}, \overline{\gamma_2}) = \frac{\pi}{2}$, and hence the path P_1 is radial by Lemma 1 (ii). Furthermore, one observe that the bar $\overline{\gamma_3}$ is contained in $F_{\gamma_1}[\frac{\pi}{2}, \frac{3\pi}{2}]$ and the bar $\overline{\gamma_4}$ is contained in $F_{\gamma_3}[\frac{\pi}{2}, \frac{3\pi}{2}]$ since $\theta(\overline{\gamma_1}, \overline{\gamma_3}) = \frac{\pi}{2}$ and $\angle\gamma_0\gamma_3\gamma_4 = \frac{3\pi}{2}$. Thus, by Lemma 1 (ii), the path P_2 is radial. □

Every C_i component is radial since all subcomponents are radial by Lemma 2 above, and hence the tree constructed in Sect. 3 is radial.

5. Lockability

In this section, we present a theorem that the tree constructed in Sect. 3 cannot be flattened. Note that the method of the proof described in [4] cannot directly apply to our tree.

For the initial configuration, the following lemma holds.

Lemma 3: The following four inequalities hold:

(i) $\angle r\gamma_1 l_1 < \frac{\pi}{2}$,
(ii) $\angle l_1\gamma_1\gamma_2 < \frac{\pi}{2}$,
(iii) $\angle r\gamma_4\gamma_3 < \frac{\pi}{2}$, and
(iv) $\angle\gamma_3\gamma_4 v_2^+ < \frac{\pi}{2}$.

Proof. Since the sum $\angle r\gamma_1 l_1 + \angle l_1\gamma_1\gamma_2$ is equal to $\angle r\gamma_1\gamma_2 (= \frac{\pi}{2})$, both (i) and (ii) immediately follow. Moreover, since the sum $\angle r\gamma_4\gamma_3 + \angle\gamma_4\gamma_3 r + \angle\gamma_3 r\gamma_4$ is equal to π and the angle $\angle\gamma_4\gamma_3 r$ is equal to $\frac{\pi}{2}$, (iii) follows. Thus, we only prove (iv) below.

A *quadrangle* is a convex polygon with four vertices A, B, C, D counterclockwise, and is denoted by $\square ABCD$. For the quadrangle $\square r\gamma_3\gamma_4\gamma_1^+$, it follows that $\angle\gamma_4\gamma_3 r = \angle r\gamma_1^+\gamma_4 (= \frac{\pi}{2})$ from our construction of the tree, and hence the sum $\angle\gamma_1^+\gamma_4\gamma_3 + \angle\gamma_3 r\gamma_1^+$ is equal to π. Let Z and W be vertices of a rectangle $\square rZW\gamma_1^+$ such that the vertex Z is on $\overline{\gamma_2}$ and the vertex W is on $\overline{\gamma_2}^+$, as illustrated in Fig. 10.

Then, the angle $\angle\gamma_1 Zr$ is equals to $\angle\gamma_1 r\gamma_1^+ (= \frac{2\pi}{n})$, since the equation $\angle Zr\gamma_1 + \angle\gamma_1 Zr = \angle Zr\gamma_1 + \angle\gamma_1 r\gamma_1^+ = \frac{\pi}{2}$ holds. Therefore, the equation $|\gamma_1^+ W| = |rZ| = \frac{1}{\sin(\frac{2\pi}{n})}$ follows. The condition $|\gamma_1^+ v_1^+| < \frac{1}{\sin(\frac{2\pi}{n})}$ holds from Eq. (1), and hence v_1^+ is on the open line segment $\gamma_1^+ W$. Since both $O(r, v_1^+)$ and $O(r, W)$ have the same chord $r\gamma_1^+$ and the radius of $O(r, v_1^+)$ is smaller than the radius of $O(r, W)$, γ_3 lies between points γ_1 and Z from the construction. On the other hand, one can easily observe that $\angle\gamma_3\gamma_4 v_2^+ = \angle\gamma_3 r\gamma_1^+$ since the equation $\angle\gamma_1^+\gamma_4\gamma_3 + \angle\gamma_3\gamma_4 v_2^+ = \angle\gamma_1^+\gamma_4\gamma_3 + \angle\gamma_3 r\gamma_1^+ = \pi$ holds.

Thus, the angle $\angle\gamma_3\gamma_4 v_2^+$ is equal to $\angle Zr\gamma_1^+$ and is smaller than $\frac{\pi}{2}$. □

For each C_i, the angle $\angle v_1 r v_1^+$ is called *the angle of* C_i and may be denoted by $\angle C_i$. A reconfiguration *widens* C_i if it makes the angle $\angle C_i$ increase, and *squeezes* C_i if it makes the angle $\angle C_i$ decrease.

The following lemmas hold.

Lemma 4: There exists a widened C_i component if and only if there exists a squeezed C_j component, where $0 \le i, j \le n-1$ and $i \ne j$.

Proof. Since the sum $\sum_{i=0}^{n-1} \angle C_i$ is equal to 2π, the claim immediately follows. □

From Lemma 3 and 4, one can observe the following Lemma holds, a proof of which will be given in Sect. 6.

Lemma 5: (i) No reconfiguration can squeeze any C_i component.
(ii) No reconfiguration can widen any C_i component.

Thus, the following theorem holds.

Theorem 1: There exists a radial tree which cannot be flattened.

6. Proof of Lemma 5

In this section, we prove Lemma 5 whose proof is omitted in Sect. 5.

We first give some additional notation. For any point $p \in \mathbb{R}^2$, the x-,y-coordinate of p is denoted by $x(p)$,$y(p)$,respectively. Recall that the circle centered at $p \in \mathbb{R}^2$ with radius $a \in \mathbb{R}$ is denoted by $O_p(a)$. An inner open region bounded by $O_p(a)$ is denoted by $\hat{O}_p(a)$, and an outer closed region bounded by $O_p(a)$ is denoted by $\breve{O}_p(a)$. Note that $\hat{O}_p(a)$ does not include any points on the boundary $O_p(a)$, but $\breve{O}_p(a)$ does. An arc on $O_p(a)$ from a point q to a point q' counterclockwise is denoted by $A_p(a; q, q')$.

Below, we regard the reconfiguration as a continuous function on time $t \in [0, \infty)$, where the initial configuration is the image of this reconfiguration at time $t = 0$. The configuration of any object o at time t is denoted by $o(t)$. For example, a configuration of joint v_1 at time t is denoted by $v_1(t)$. Moreover,$C_i(0) = C_i^*$ for every i, $0 \le i \le n-1$. We use similar notation for the others.

We may assume, without loss of generality, that the root r is located on the origin of the xy-plane, and the bar $\overline{v_1}$ of C_0 is fixed during any time $t \in [0, \infty)$ for any reconfiguration. Thus, for any time $t \in [0, \infty)$ of any reconfiguration, the following equation holds:

$$\overline{v_1}(t) = \overline{v_1}(0) (= \overline{v_1}^*). \qquad (2)$$

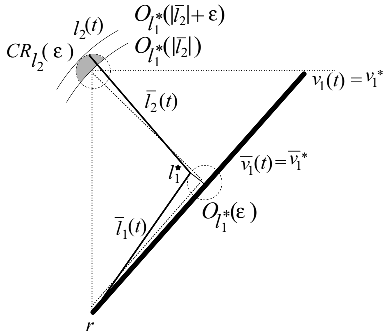

Fig. 11 Feasible position of l_2 in time $[0, \delta)$.

Therefore, the following equations also hold:

$$\begin{cases} v_0(t) = v_0(0) (= v_0^* = r), \\ v_1(t) = v_1(0) (= v_1^*). \end{cases}$$

We shall prove some lemmas before proving Lemma 5.

In order to prove these lemmas, we consider *infinitely small motion* of linkage. We say that a motion of linkage $L = (J, B)$ is *infinitely small* for $\varepsilon > 0$ and $t > 0$ if every joint $j \in J$ is contained in $\hat{O}_{j(0)}(\varepsilon)$ during period $[0, t)$. Since every reconfiguration is continuous, for any small real number $\varepsilon > 0$, there exists a time $\delta > 0$ such that the reconfiguration is infinitely small for ε and δ, i.e., every joint $j \in J$ is properly contained in $\hat{O}_{j(0)}(\varepsilon)$ during period $[0, \delta)$. Below, we only consider such infinitely small motion for a sufficiently small ε and a corresponding short time δ, so that no critical event occur, like $s(\overline{\gamma_4}(t)) - s(\overline{v_2}^+(t)) = \frac{\pi}{2}$.

A *crescent region* $CR_j(\varepsilon)$ is the region defined by $\hat{O}_{j^*}(\varepsilon) \cap \breve{O}_{j'^*}(|\overline{j}|)$, where j' is the parent joint of j. The following lemmas hold.

Lemma 6: For any reconfiguration, the following membership holds during any time $t \in [0, \delta)$:

$$l_2(t) \in CR_{l_2}(\varepsilon).$$

Proof. From the assumption of infinitely small motion, $l_2(t)$ is contained in $\hat{O}_{l_2^*}(\varepsilon)$. Thus, we shall only show that $l_2(t) \in \breve{O}_{l_1^*}(|\overline{l_2^*}|)$.

Let $l_1^\star$ be the intersection of $O_{l_1^*}(\varepsilon)$ and $O_r(|\overline{l_1}|)$ satisfying $s(rl_1^\star) < s(rl_1^*)$. (See Fig. 11.) Since $l_0 (= r)$ is fixed for any reconfiguration and any time, $l_1(t)$ should lie on $O_r(|\overline{l_1}|)$. Moreover, the angle $\angle v_1(t) r l_1(t)$ should be greater than or equal to zero at any time $t \in [0, \delta)$ from Eq.(2) and the condition of a non-crossing reconfiguration. Thus, $l_1(t)$ should lie on $A_r(|\overline{l_1}|; l_1^*, l_1^\star)$ during time $t \in [0, \delta)$.

Furthermore, joint $l_2(t)$ should lie on $O_{l_1(t)}(|\overline{l_2}|)$. Let R be the region swept by a part of $\breve{O}_{l_1(t)}(|\overline{l_2}|)$ with center from l_1^* to $l_1^\star$ on $A_r(|\overline{l_1}|; l_1^*, l_1^\star)$. Then, at any time $t \in [0, \delta)$, joint $l_2(t)$ is contained in R.

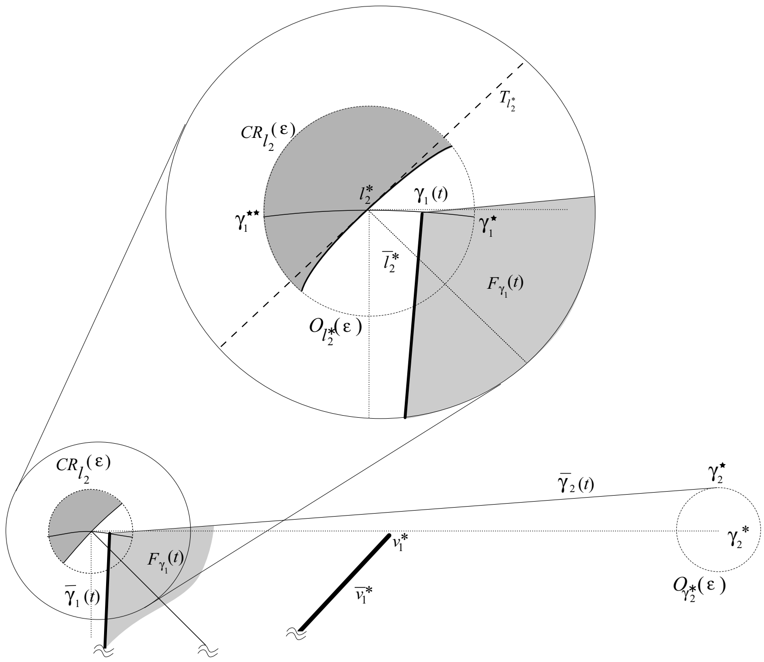

Fig. 12 Impossible motion of γ_1.

One can easily observe that the region R contained in $\check{O}_{l_1^*}(|\overline{l_2}|) \cap \hat{O}_{l_1^*}(|\overline{l_2}| + \varepsilon)$.

Thus,the claim holds. □

Lemma 7: For any reconfiguration, the following inequality holds at any time $t \in [0, \delta)$:

$$\angle v_1^* r \gamma_1(t) \geq \angle v_1^* r \gamma_1(0).$$

Proof. By Eq.(2), it is sufficient to show that the slope $s(\overline{\gamma_1}(t))$ is greater than or equal to $\frac{\pi}{2}$.

Suppose for a contradiction that $s(\overline{\gamma_1}(t))$ is smaller than $\frac{\pi}{2}$ for some time $t \in [0, \delta)$.

Let $\gamma_1(t)\gamma_2^\star$ be the upper tangent of point $\gamma_1(t)$ and circle $O_{\gamma_2^*}(\varepsilon)$, and let $F_{\gamma_1}(t)$ be a fan $r\gamma_1(t)\gamma_2^\star$, as illustrated in Fig. 12.

Then, one can observe that $l_2(t)$ should be contained in $F_{\gamma_1}(t)$ from the condition of a non-crossing reconfiguration since no critical events occur during $[0, \delta)$. On the other hand, by Lemma 6, $l_2(t)$ should be contained in $CR_{l_2}(\varepsilon)$. We shall show below that the equation $F_{\gamma_1}(t) \cap CR_{l_2}(\varepsilon) = \emptyset$ holds.

Let $\gamma_1^\star$ and $\gamma_1^{\star\star}$ be two intersections of $O_{\gamma_1}(\varepsilon)$ and $O_r(|\overline{\gamma_1}|)$ satisfying $s(r\gamma_1^\star) < s(r\gamma_1^{\star\star})$, and let $T_{l_2^*}$ be the tangent of $O_{l_1^*}(|\overline{l_2}|)$ at l_2^*, as illustrated in Fig. 12. Then, $T_{l_2^*}$ is perpendicular to bar $\overline{l_2^*}$. Moreover, by Lemma 3, the angle $\angle r\gamma_1^* l_1^*$ is smaller than $\frac{\pi}{2}$ and the angle $\angle l_1^* \gamma_1^* \gamma_2^*$ is also smaller than $\frac{\pi}{2}$, and hence the equation $F_{\gamma_1}(0) \cap CR_{l_2}(\varepsilon) = \{\gamma_1^*\}$ holds at time $t = 0$. Furthermore, $\gamma_1(t)$ should lie on $A_r(|\overline{\gamma_1}|; \gamma_1^\star, \gamma_1^*)$, and hence $x(\gamma_1(t))$ is greater than zero since the slope $s(\overline{\gamma_1}(t))$ is smaller than $\frac{\pi}{2}$. This means that $F_{\gamma_1}(t) \cap CR_{l_2}(\varepsilon) = \emptyset$ at time $t > 0$. □

Lemma 8: For any reconfiguration, the following inequality holds during the time $t \in [0, \delta)$:

$$s(\overline{\gamma_2}(t)) \geq 0.$$

Proof. By the proof of Lemma 7, one can observe that $\gamma_1(t)$ should lie on $A_r(|\overline{\gamma_1}|; \gamma_1^*, \gamma_1^{\star\star})$. The y-coordinate of any point on $A_r(|\overline{\gamma_1}|; \gamma_1^*, \gamma_1^{\star\star})$ is smaller than or equal to $y(\gamma_1^*)(=1)$. Moreover, $\overline{\gamma_2}(t)$ should be above v_1^* whose y-coordinate is equal to $y(v_1^*)(=1)$ from Eq.(2), and $\gamma_2(t)$ should be contained in $\hat{O}_{\gamma_2^*}(\varepsilon)$. Thus, the claim should hold from the condition of a non-crossing reconfiguration. □

Lemma 9: For any reconfiguration, if $\overline{\gamma_2}$ is fixed during the time $t \in [0, \delta)$ then the following inequality holds:

$$\angle \gamma_1^* r v_1^+(t) \geq \angle \gamma_1^* r v_1^+(0).$$

Proof. Assume that $\overline{\gamma_2}$ is fixed during the time $t \in [0, \delta)$ in this proof. Then, it is sufficient to show that $s(\overline{v_1}^+(t)) \geq s(\overline{v_1}^+(0))$.

Suppose for a contradiction $s(\overline{v_1}^+(t)) < s(\overline{v_1}^+(0))$ for some time $t \in [0, \delta)$. Let $\gamma_3^\star$ be the intersection of $O_{\gamma_3^*}(\varepsilon)$ and $O_{\gamma_1^*}(|\overline{\gamma_3}|)$ satisfying $s(\gamma_1^* \gamma_3^\star) > 0$, as illustrated in Fig. 13.

Since γ_1^* and $\overline{\gamma_2}^*$ are fixed, $\gamma_3(t)$ should lie on $A_{\gamma_1^*}(|\overline{\gamma_3}|; \gamma_3^*, \gamma_3^\star)$. Similarly to the proof of Lemma 6, one can easily observe that the following membership holds:

$$\gamma_4(t) \in CR_{\gamma_4}(\varepsilon).$$

Let $F_{v_1^+}(t)$ be the fan $rv_1^+(t)v_2^+(t)$. Then, similarly to the proof of Lemma 7, one can observe that

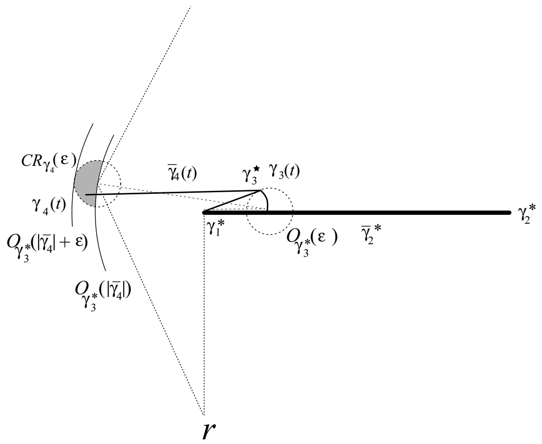

Fig. 13 Feasible position of γ_4 in time $[0, \delta)$.

$F_{v_1^+}(t) \cap CR_{\gamma_4}(\varepsilon) = \emptyset$ as follows. By Lemma 3, the angle $\angle r v_1^{+*} \gamma_3^*$ is smaller than $\frac{\pi}{2}$ and the angle $\angle \gamma_3^* \gamma_1^{+*} v_2^{+*}$ is also smaller than $\frac{\pi}{2}$, and hence the equation $F_{v_1^+}(0) \cap CR_{\gamma_4}(\varepsilon) = \{\gamma_4^*\}$ holds at time $t = 0$. However, since the slope $s(\overline{v_1}^+(t))$ is smaller than $s(\overline{v_1}^{+*})$, the equation $F_{v_1^+}(t) \cap CR_{\gamma_4}(\varepsilon) = \emptyset$ follows at time $t > 0$. □

We are now ready to prove Lemma 5.

Proof of Lemma 5 By Lemma 4, it is sufficient to show only (i), i.e., we shall only show that no reconfiguration can squeeze any C_i component.

By Lemma 9, the angle $\angle v_1^* r v_1^+(t)$ is greater than or equal to $\angle v_1^* r v_1^+(0)$ if $\overline{\gamma_2}$ is fixed during the time $t \in [0, \delta)$. Moreover, since the inequality $x(\gamma_1(t)) \leq x(\gamma_1^*)$ holds by Lemma 7 and the inequality $s(\overline{\gamma_2}(t)) \geq 0$ holds by Lemma 8, the x-coordinate $x(\gamma_3(t))$ is smaller than or equal to $x(\gamma_3^*)$. This means that $v_1^+(t)$ should be contained in the region obtained by shifting $CR_{\gamma_4}(\varepsilon)$ to the $-x$ direction. Therefore, the angle $\angle v_1^* r v_1^+(t)$ is greater than or equal to $\angle v_1^* r v_1^+(0)$ even if $\gamma_1(t)$ rotates about the center r counterclockwise.

Thus, the claim holds. □

7. Conclusion

In this paper, we show that there exists a tree linkage which is radially monotone and cannot be flattened. The following future works remain:

(1) find new characterization of a class of tree linkages which can be flattened,
(2) find a method for flattening a class of tree linkages other than monotone trees, and
(3) find other necessary or sufficient conditions for linkages to be reconfigured to some regular form, say, straightened, flattened, or convexified,$\cdots$.

Acknowledgments

We would like to thank Dr. Takao Nishizeki and Dr. Akiyoshi Shioura in Tohoku University for their helpful comments, which improve the presentation of this paper. We also wish to thank anonymous referees for their valuable comments, which improve the clarity of this paper.

References

[1] H. Alt, C. Knauer, G. Rote, and S. Whitesides, “On the complexity of the linkage reconfiguration problem” in Towards a Theory of Geometric Graphs, American Mathematical Society, pp.1–14, 2004. A preliminary version appeared as, “The complexity of (un)folding,” Proc. 19th ACM Symp. Computational Geometry, pp.164–170, 2003.

[2] T. Biedl, E. Demaine, M. Demaine, S. Lazard, A. Lubiw, J. O’Rourke, S. Robbins, I. Streinu, G. Toussaint, and S. Whitesides, “A note on reconfiguring tree linkages: Trees can lock,” Discrete Applied Mathematics, vol.254, pp.19–32, 2002. A preliminary version appeared in Proc. 10th Canadian Conference on Computational Geometry, 1998.

[3] R. Connelly, E. Demaine, and G. Rote, “Straightening polygonal arcs and convexifying polygonal cycles,” Discrete and Computational Geometry, vol.30, pp.205–239, 2003. A preliminary version appeared in Proc. 41st IEEE Symp. Foundations of Computer Science, pp.432–442, 2000.

[4] R. Connelly, E. Demaine, and G. Rote, “Infinitesimally locked self-touching linkages with applications to locked trees,” Physical Knots: Knotting, Linking, and Folding Geometric Objects in R^3, American Mathematical Society, pp. 287-311, 2002. A preliminary version appeared in Proc. 11th Annual Fall Workshop on Computational Geometry, 2001.

[5] Y. Kusakari, M. Sato, and T. Nishizeki, “Planar reconfiguration of monotone trees,” IEICE Trans. Fund., Vol.E85-A, No.5, pp.938-943, May 2002.

[6] Y. Kusakari, “On Reconfiguring radial trees,” Proc. JCDCG2002, Lecture Notes in Computer Science, 2866, Springer-Verlag, pp.182–191, 2003.

[7] J. O’Rourke, “Folding and unfolding in computational geometry,” Proc. JCDCG ’98, Lecture Notes in Computer Science, 1763,Springer-Verlag, pp.258–266, 2000.

[8] I. Streinu, “A combinatorial approach to planar non-colliding robot arm motion planning,” Proc. 41st IEEE Symp. Foundations of Computer Science, pp.443–453, 2000.

Yoshiyuki Kusakari received the B.E. degree in information engineering, and the M.S. and Ph.D. degrees in information science from Tohoku University, Japan, in 1993, 1995 and 1998, respectively. He joined Akita Prefectural University in 2000, and is currently Associate Professor of Faculty of Systems Science and Technology. His research interests include graph theory and computational geometry.